An adaptive multi-element generalized polynomial chaos method for stochastic differential equations

Xiaoliang Wan, George Em Karniadakis *

Division of Applied Mathematics, Center for Fluid Mechanics, Brown University, 182 George Street, Box F, Providence, RI 02912, USA

Abstract

We formulate a Multi-Element generalized Polynomial Chaos (ME-gPC) method to deal with long-term integration and discontinuities in stochastic differential equations. We first present this method for Legendre-chaos corresponding to uniform random inputs, and subsequently we generalize it to other random inputs. The main idea of ME-gPC is to decompose the space of random inputs when the relative error in variance becomes greater than a threshold value. In each subdomain or random element, we then employ a generalized polynomial chaos expansion. We develop a criterion to perform such a decomposition adaptively, and demonstrate its effectiveness for ODEs, including the Kraichnan–Orszag three-mode problem, as well as advection–diffusion problems. The new method is similar to spectral element method for deterministic problems but with h–p discretization of the random space.
© 2005 Elsevier Inc. All rights reserved.

Keywords: Uncertainty; Polynomial chaos; Discontinuities

1. Introduction

Polynomial chaos is a non-statistical approach to represent randomness and is based on the homogeneous chaos theory of Wiener [1]. In its original form a spectral expansion was employed based on the Hermite orthogonal polynomials in terms of Gaussian random variables. This expansion was applied by Ghanem et al. [2,3] to various problems in mechanics. A broader framework, called "generalized Polynomial Chaos (gPC)", was introduced in [4,5]. This extension includes a family of orthogonal polynomials (the so-called Askey scheme) from which the trial basis is selected, and can represent non-Gaussian processes more efficiently; it includes the classical Hermite polynomial chaos as a subset. For example, uniform

distributions are represented by Legendre polynomial functionals, exponential distributions by Laguerre polynomial functionals, etc. The method includes also *discrete* distributions with corresponding *discrete* eigenfunctions as trial basis; e.g., Poisson distributions are represented by Charlier polynomial functionals.

More specifically, stochastic ordinary differential equations (ODEs) were considered in [4] and gPC was shown to exhibit exponential convergence in approximating stochastic solutions at finite (early) times. However, the absolute error may increase gradually in time and become unacceptably large for long-term integration. Increasing the polynomial order adaptively can somewhat alleviate this problem, however, the stochastic solution may become increasingly complicated, which may give rise to serious computational difficulties. For example, if the stochastic solutions are periodic with random frequencies, gPC will lose its effectiveness rapidly due to the amplified phase shift with time. The same is true for time-dependent simulations of fluid flows, which are the problems considered in [5]. In addition, for discontinuous dependence of the solution on the input random data, gPC may converge slowly or fail to converge even in short-time integration. This situation represents essentially a discontinuity of the approximated solution in random space, for which global solutions converge slowly. Therefore, more efficient and robust schemes are needed to enhance the performance of generalized as well as the original polynomial chaos. To this end, a new method, termed the Wiener–Haar method, was developed in [6,7] based on wavelets; its primary aim was to address problems related to the aforementioned discontinuities in random space.

In this paper, we develop a *simple* but effective scheme based on gPC, i.e., we maintain a *spectral* polynomial trial basis. It is motivated by two observations:

(1) gPC is more efficient for relatively small degree of random perturbation, and
(2) most of the statistics we are interested in, such as mean and variance, are defined as integrations involving the probability density function (PDF).

To this end, we decompose the space of random inputs into small elements. Subsequently, in each element we generate a new random variable and apply gPC again. Since the degree of perturbation in each element is reduced proportionally to the size of random elements, we can maintain a relative low polynomial order for gPC in each element. This multi-element gPC method (ME-gPC) can achieve h–p convergence (as in spectral elements for spatial discretization), where h is determined by the size of random elements and p is the polynomial chaos order. The concept of h-convergence used in this work is similar to that in [8], where the basis of the standard finite element method is employed. In ME-gPC, orthogonal basis (Legendre-chaos) is used in each random element for efficiency. By extension, we can say that in [6,7] the concept of h-convergence is also used with h representing the number of resolution levels of wavelets. From the implementation standpoint, the simplicity of ME-gPC is particularly attractive; for example, we do not have to change the existing gPC solver except for a subroutine for the decomposition of random space. As we shall see in this paper, however, the results are dramatically improved compared to global gPC expansions.

This paper is organized in the following way. In the next section, we recall the basic concepts and properties of gPC. Then, we introduce the ME-gPC algorithm and the criterion of the decomposition of random space in Section 3. In Section 4, we study the properties of ME-gPC numerically for several typical ODE and PDE problems, including the open Kraichnan–Orszag three-mode problem. A summary is included in Section 5.

2. Generalized polynomial chaos

The original polynomial chaos formulation was proposed by Wiener [1]. It employs Hermite polynomials in terms of Gaussian random variables as the trial basis to represent stochastic processes. According to

the theorem of Cameron and Martin [9] such expansions converge for any second-order processes in the L_2 sense. The gPC extension was proposed in [5] and employs more types of orthogonal polynomials from the Askey scheme. It is a generalization of the Wiener's Hermite-chaos and can deal with non-Gaussian random inputs more efficiently.

Let $(\Omega, \mathscr{F}, P)$ be a complete probability space, where Ω is the sample space, $\mathscr{F}$ is the σ-algebra of subsets of Ω, and P is a probability measure. A general *second-order* random process $X(\omega) \in L_2(\Omega, \mathscr{F}, P)$ can be expressed by gPC as

$$X(\omega) = \sum_{i=0}^{\infty} \hat{a}_i \Phi_i(\boldsymbol{\xi}(\omega)), \tag{1}$$

where ω is the random event and $\Phi_i(\boldsymbol{\xi}(\omega))$ are polynomial functionals of degree p in terms of the multi-dimensional random variable $\boldsymbol{\xi} = (\xi_1, \ldots, \xi_d)$. The family $\{\Phi_i\}$ is an orthogonal basis in $L_2(\Omega, \mathscr{F}, P)$ with orthogonality relation

$$\langle \Phi_i, \Phi_j \rangle = \langle \Phi_i^2 \rangle \delta_{ij}, \tag{2}$$

where δ_{ij} is the Kronecker delta, and $\langle \cdot, \cdot \rangle$ denote the ensemble average. Here, the ensemble average can be defined as the inner product in the Hilbert space in terms of the random vector $\boldsymbol{\xi}$,

$$\langle f(\boldsymbol{\xi}), g(\boldsymbol{\xi}) \rangle = \int f(\boldsymbol{\xi}) g(\boldsymbol{\xi}) w(\boldsymbol{\xi}) \mathrm{d}\boldsymbol{\xi} \tag{3}$$

or

$$\langle f(\boldsymbol{\xi}), g(\boldsymbol{\xi}) \rangle = \sum_{\boldsymbol{\xi}} f(\boldsymbol{\xi}) g(\boldsymbol{\xi}) w(\boldsymbol{\xi}) \tag{4}$$

in the discrete case, where $w(\boldsymbol{\xi})$ denotes the weight function.

For a certain random vector $\boldsymbol{\xi}$, the gPC basis $\{\Phi_i\}$ can be selected in such a way that its weight function has the *same* form as the probability distribution function of $\boldsymbol{\xi}$. The corresponding type of polynomials $\{\Phi_i\}$ and their associated random variable $\boldsymbol{\xi}$ can be found in [4].

3. Multi-element generalized polynomial chaos

In this section, we develop the scheme of Multi-Element generalized Polynomial Chaos (ME-gPC) to maintain the high accuracy of gPC for *long-term integration* and to resolve effectively *discontinuities* in random space.

3.1. Decomposition of random space

Let $\boldsymbol{\xi} = (\xi_1(\omega), \xi_2(\omega), \ldots, \xi_d(\omega))$: $\Omega \mapsto \mathbb{R}^d$ denote a d-dimensional random vector defined on the probability space $(\Omega, \mathscr{F}, P)$, where ξ_i are identical independent distributed (IID) random variables. Here we assume that ξ_i are also *uniform* random variables defined as $\xi_i: \Omega \mapsto [-1, 1]$ with a constant PDF $f_i = \frac{1}{2}$.

Let **D** be a decomposition of B with N non-overlapping elements

$$\mathbf{D} = \begin{cases} B_k = [a_1^k, b_1^k) \times [a_2^k, b_2^k) \times \cdots \times [a_d^k, b_d^k], \\ B = \bigcup_{k}^{N} B_k, \\ B_{k_1} \bigcap B_{k_2} = \emptyset \quad \text{if } k_1 \neq k_2, \end{cases} \tag{5}$$

where $k, k_1, k_2 = 1, 2, \ldots, N$. We define an *indicator* random variable for each random element as

$$z_k = \begin{cases} 1 & \text{if } \boldsymbol{\xi} \in B_k, \\ 0 & \text{otherwise.} \end{cases} \tag{6}$$

It is easy to see that $\Omega = \bigcup_{k=1}^{N} z_k^{-1}(1)$ and $z_i^{-1}(1) \cap z_j^{-1}(1) = \emptyset$ when $i \neq j$. Thus, $\bigcup_{k=1}^{N} z_k^{-1}(1)$ is a decomposition of the sample space Ω. Then, in each random element we define the following local random vector as

$$\boldsymbol{\zeta}^k = (\zeta_1^k, \zeta_2^k, \ldots, \zeta_d^k): z_k^{-1}(1) \mapsto B_k \tag{7}$$

subject to a conditional PDF

$$f_{\zeta^k} = \frac{1}{2^d \Pr(z_k = 1)}, \quad k = 1, 2, \ldots, N, \tag{8}$$

where

$$\Pr(z_k = 1) = \prod_{i=1}^{d} \frac{b_i^k - a_i^k}{2}. \tag{9}$$

Note that $\Pr(z_k = 1) > 0$. Subsequently, we map $\boldsymbol{\zeta}^k$ to a new random vector defined in $[-1, 1]^d$,

$$\boldsymbol{\xi}^k = g_k(\boldsymbol{\zeta}^k) = (\xi_1^k, \xi_2^k, \ldots, \xi_d^k) : z_k^{-1}(1) \mapsto [-1, 1]^d \tag{10}$$

with a constant PDF $f^k = (\frac{1}{2})^d$, where

$$g_k(\boldsymbol{\zeta}^k): \zeta_i^k = \frac{b_i^k - a_i^k}{2} \xi_i^k + \frac{b_i^k + a_i^k}{2}, \quad i = 1, 2, \ldots, d. \tag{11}$$

To this end, we present a decomposition of the random space of $\boldsymbol{\xi}$. Given a system of differential equations with random inputs $\boldsymbol{\xi}$, the output $u(\boldsymbol{\xi})$ is also measurable on the probability space $(\Omega, \mathscr{F}, P)$. Thus, we can express $u(\boldsymbol{\xi})$ in each random element using $\boldsymbol{\zeta}^k$ subject to a conditional PDF, which implies that we can first approximate $u(\boldsymbol{\xi})$ locally by $\boldsymbol{\zeta}^k$ on the probability space $(z_k^{-1}(1), \mathscr{F} \cap z_k^{-1}(1), P(\cdot | z_k^{-1}(1)))$, then combine all the information from each random element to get $u(\boldsymbol{\xi})$ in the whole random space. Since most of the statistics are integrations with respect to the PDF, we do not have to guarantee the absolute continuity in terms of $\boldsymbol{\xi}$ between random elements. In other words, the following restriction:

$$u_{B_1}(\boldsymbol{\xi}) = u_{B_2}(\boldsymbol{\xi}), \quad \boldsymbol{\xi} \in \bar{B}_1 \cap \bar{B}_2, \tag{12}$$

where $\bar{B}_1$ and $\bar{B}_2$ indicate the closure of two adjacent random elements, respectively, is not required as in the deterministic problems since the measure of the interface is zero. Thus, in random element k we can use gPC locally to solve the system of differential equations with random inputs $\boldsymbol{\zeta}^k$ instead of $\boldsymbol{\xi}$. According to the theorem of Cameron and Martin [9], gPC will converge to $u(\boldsymbol{\zeta}^k)$ in the L_2 sense. Hence, we decompose the original problem to N independent problems in N random elements.

In practice we implement gPC according to $\boldsymbol{\xi}^k$ instead of $\boldsymbol{\zeta}^k$ to take advantage of the Legendre-chaos. After we obtain the approximation $\hat{u}_k(\boldsymbol{\xi}^k)$, $k = 1, 2, \ldots, N$, of a random field, we can reconstruct the mth moment of $u(\boldsymbol{\xi})$ on the entire random domain by the Bayes' theorem and the law of total probability [10]

$$\mu_m(u(\boldsymbol{\xi})) = \int_B u^m(\boldsymbol{\xi}) \left(\frac{1}{2}\right)^d \mathrm{d}\boldsymbol{\xi} \approx \sum_{k=1}^{N} \Pr(z_k = 1) \int_{[-1,1]^d} \hat{u}_k^m(\boldsymbol{\xi}^k) \left(\frac{1}{2}\right)^d \mathrm{d}\boldsymbol{\xi}^k. \tag{13}$$

Since we consider second-order processes in this work, $m = 1, 2$. For convenience, we use J_k to denote $\Pr(z_k = 1)$ in the presentation below.

3.2. Accuracy

Theorem 1. *Suppose ξ is a random vector defined on $[-1,1]^d$ with IID uniform components. If the random space of ξ is decomposed into N disjoint elements with each element k described by a new uniform random vector ξ^k (see Eq. (10)), the mth (m = 1, 2) moment of random field $u(\xi) \in L_2(\Omega, \mathcal{F}, P)$ can be approximated by $\hat{u}_k(\xi^k)$, $k = 1, 2, \ldots, N$, with a L_2 error*

$$\epsilon = \left(\sum_{k=1}^{N} \epsilon_k^2 J_k \right)^{1/2}, \tag{14}$$

where ϵ_k is the local L_2 error of the mth moment in random element k, $J_k = \Pr(z_k = 1)$ and $\hat{u}_k(\xi^k)$ is obtained from gPC.

Proof. Let $\hat{u}(\xi)$ be the approximate random field. We first assume that the *m*th moment of $\hat{u}(\xi)$ takes the form

$$\hat{u}^m(\xi) = \sum_{k=1}^{N} \hat{u}_k^m(g_k(\xi)) z_k, \tag{15}$$

since $B = \cup_{i=1}^{N} B_i$, $\zeta^i \in B_i$ and $\xi \in B$ (see Eqs. (7) and (11)). Then,

$$\epsilon^2 = \int_B \left(u^m(\xi) - \sum_{k=1}^{N} \hat{u}_k^m(g_k(\xi)) z_k \right)^2 \left(\frac{1}{2} \right)^d \mathrm{d}\xi = \sum_{k=1}^{N} \Pr(\xi \in B_k) \int_{B_k} \left(u^m(\zeta^k) - \hat{u}_k^m(g_k(\zeta^k)) \right)^2 f_{\zeta_k} \mathrm{d}\zeta^k$$

$$= \sum_{k=1}^{N} \Pr(\xi \in B_k) \int_{[-1,1]^d} \left(u^m(g_k^{-1}(\xi^k)) - \hat{u}_k^m(\xi^k) \right)^2 \left(\frac{1}{2} \right)^d \mathrm{d}\xi^k = \sum_{k=1}^{N} \epsilon_k^2 J_k.$$

For the second step, we employ the Bayes' theorem and the law of total probability [10]. If gPC is employed to approximate $u(g_k^{-1}(\xi^k))$, ϵ_k goes to zero according to the theorem given by Cameron and Martin [9]. Since $\sum_{k=1}^{N} J_k = 1$, ϵ also goes to zero. Note here that although we approximate the random field locally we can rebuild the global random field by Eq. (15). □

Note that $\sum_{k=1}^{N} J_k = 1$. Thus ϵ^2 is a weighted mean of ϵ_k^2, $k = 1, 2, \ldots, N$. From the transform (11) we can see that the degree of random perturbation for each dimension of ξ^k is scaled down from O(1) to $O(\frac{b_i^k - a_i^k}{2})$. This means that the decomposition of random space can effectively decrease the degree of randomness. Thus, for the same polynomial order any ϵ_k would be smaller than the error given by gPC on the entire random space without the decomposition of random space.

In [8] error estimates were derived for the *mean* and the *variance* for a similar decomposition of random space in the framework of deterministic finite element method, as follows:

$$|\bar{u} - \bar{\hat{u}}| \leqslant C_1(p) O(h^{2(p+1)}), \quad |\sigma^2 - \hat{\sigma}^2| \leqslant C_2(p) O(h^{2(p+1)}), \tag{16}$$

where the element size $h \propto N^{-1}$ in our case and p is the polynomial order. In [8], the same basis as the deterministic finite element is employed to approximate the random field, where the accuracy mainly relies on the decomposition of random space. In ME-gPC, we employ Legendre-chaos locally to take advantage of orthogonality and related efficiencies.

Let us now return to the two specific problem we aim to address in this paper: *discontinuity* and *long-term integration*. If a discontinuity exists in random space, then gPC may converge very slowly or give rise to O(1) error. However, ME-gPC can overcome this difficulty. Let us assume that the discontinuity occurs in the random element k. From Eq. (14) we can see that the error contribution of element k is $\epsilon_k^2 J_k$, which is

determined by the local approximation error in element k and the factor J_k together. So the error contribution can be decreased by the factor J_k (dictated by the element size) even if the local approximation error is big. Thus, we can maintain a high accuracy on the entire random domain by using bigger elements for the smooth part (p-type convergence) and smaller elements for the discontinuous part (h-type convergence). To control the error in long-term integration problems, one choice is to increase the polynomial order adaptively. However, the stochastic system will become bigger, which may lead to a complicated system of deterministic differential equations with all stochastic modes coupled together, especially in problems with high-order nonlinearity. In ME-gPC, we can use a relative low polynomial order in each random element since the local degree of perturbation has been scaled down; thus, the complexity is effectively controlled. In practice, the polynomial order cannot be increased arbitrarily high, which means that the range of application of gPC is indeed limited. It is obvious that such a range can be effectively extended by the decomposition of random space.

3.3. Adaptive criterion

Let us assume that the gPC expansion of random field in element k is

$$\hat{u}_k(\xi^k) = \sum_{i=0}^{N_p} \hat{u}_{k,i} \Phi_i(\xi^k), \tag{17}$$

where p is the highest order of polynomial chaos and N_p denotes the total number of basis modes given by

$$N_p = \frac{(p+d)!}{p!d!} - 1. \tag{18}$$

The *approximate global mean* can be expressed as

$$\bar{u} = \sum_{k=1}^{N} \hat{u}_{k,0} J_k. \tag{19}$$

From the orthogonality of gPC we can obtain the *local variance* approximated by polynomial chaos with order p

$$\sigma_{k,p}^2 = \sum_{i=1}^{N_p} \hat{u}_{k,i}^2 \langle \Phi_i^2 \rangle, \tag{20}$$

and the *approximate global variance*

$$\bar{\sigma}^2 = \sum_{k=1}^{N} [\sigma_{k,p}^2 + (\hat{u}_{k,0} - \bar{u})^2] J_k. \tag{21}$$

Let γ_k be the error of the term $\sigma_{k,p}^2 + (\hat{u}_{k,0} - \bar{u})^2$. We obtain the *exact global variance* as

$$\sigma^2 = \bar{\sigma}^2 + \sum_{k=1}^{N} \gamma_k J_k, . \tag{22}$$

We define the local *decay rate* of relative error of the gPC approximation in each element as follows:

$$\eta_k = \frac{\sum_{i=N_{p-1}+1}^{N_p} \hat{u}_{k,i}^2 \langle \Phi_i^2 \rangle}{\sigma_{k,p}^2}. \tag{23}$$

For h-type refinement, we consider two factors: the decay rate of the relative error η_k in each element and the factor J_k. We will split a random element into two equal parts when the following condition is satisfied

$$\eta_k^\alpha J_k \geqslant \theta_1, \quad 0 < \alpha < 1, \tag{24}$$

where α is a prescribed constant.

When the random elements become smaller (i.e., J_k becomes smaller), the value of η_k satisfying the criterion will be bigger. Thus, the criterion relaxes the restriction on the accuracy of the local variance for smaller elements since the error contribution of small random elements will be dictated by their size. From Eq. (22) we can see that to achieve a certain level of accuracy, say β, we need $\sum_{k=1}^N \gamma_k J_k / \sigma^2 \sim O(\beta)$. However, it is difficult to estimate such a global error since it is related to both h-type convergence and p-type convergence. By noting the hierarchical structure of orthogonal polynomial chaos basis, we replace γ_k / σ^2 with η_k and use $\eta_k J_k$ as an indicator of the error contribution of each element in this work.

There are two reasons to use the power of η_k with respect to α in the criterion:

(1) The decomposition of random space would terminate when $J_k \sim \theta_1$. From the criterion, we can see that η_k must satisfy $\eta_k \geqslant (\theta_1 / J_k)^{1/\alpha}$ to trigger the decomposition of random space. If $J_k < \theta_1$, η_k must be greater than 1 and increase quickly as J_k becomes smaller further by noting that both θ_1 / J_k and $1/\alpha$ are greater than 1. It is, in general, hard to reach such a large η_k in practice, even for problems involving stochastic discontinuities. Thus, θ_1 acts as a limit of the size of random elements. In this paper, we usually set α to be 1/2.

(2) In stochastic discontinuity problems the largest error contribution is $\eta_k J_k \sim O(J_k) \sim O(\theta_1)$ because the relative error η_k could be almost $O(1)$ in the elements containing discontinuities. For such a case, we have to keep the error contribution of $O(\theta_1)$ because it is the best that gPC can do; however, we can eliminate the error contribution of random elements without discontinuities. Note that $\eta_k J_k \sim O(\eta_k^{1-\alpha} \theta_1)$, where θ_1 is weighted by $\eta_k^{1-\alpha}$. Thus, in random elements without discontinuities the error contribution will be much smaller than θ_1 since $\eta_k < 1$ in these elements. Finally, the total error contribution $\sum_{k=1}^N \eta_k J_k$ would be $O(m J_k) \sim O(m \theta_1)$, where m is the number of random elements with $O(\theta_1)$ error contribution. So, $\eta_k^{1-\alpha}$ works as a filter and θ_1 also acts as an accuracy threshold besides the aforementioned limit of element size.

Furthermore, we use another threshold parameter θ_2 to choose the most sensitive *random dimension*. We define the *sensitivity* of each random dimension as

$$r_i = \frac{(\hat{u}_{i,p})^2 \langle \Phi_{i,p}^2 \rangle}{\sum_{j=N_{p-1}+1}^{N_p} \hat{u}_j^2 \langle \Phi_j^2 \rangle}, \quad i = 1, 2, \ldots, d, \tag{25}$$

where we drop the subscript k for clarity and the subscript $\cdot_{i,p}$ denotes the mode consisting only of random dimension ξ_i with polynomial order p. All random dimensions which satisfy

$$r_i \geqslant \theta_2 \cdot \max_{j=1,\ldots,d} r_j, \quad 0 < \theta_2 < 1, \ i = 1, 2, \ldots, d, \tag{26}$$

will be split into two equal random elements in the next time step while all other random dimensions will remain unchanged. Hence, we can reduce the total element number while gaining efficiency. Considering that h-type refinement is efficient in practice, we only present results given by h-type refinement in this work. For some cases, say stochastic discontinuity problems, h-type refinement may be the most effective choice since p-type convergence may not be maintained anymore. This is, of course, not surprising given what we know for deterministic problems [11].

3.4. Numerical implementation

When *h*-type refinement is needed, we have to map the random field from one mesh of elements to a new mesh of elements. Suppose that the gPC expansion of the current random field is

$$\hat{u}(\hat{\xi}) = \sum_{i=0}^{N_P} \hat{u}_i \Phi_i(\hat{\xi}), \tag{27}$$

then we assume that the gPC expansion in the next level takes the following form:

$$\tilde{u}(\tilde{\xi}) = \tilde{u}\left(g\left(\hat{\xi}\right)\right) = \sum_{i=0}^{N_p} \tilde{u}_i \Phi_i(\tilde{\xi}), \tag{28}$$

where $\tilde{\xi} \in [-1, 1]^d$. To determine the (N_p+1) coefficients $\tilde{u}_i$, we choose $(N_p + 1)$ points $\tilde{\xi}_i$, $i = 0, 1, \ldots, N_p$, which are the uniform grid points in $[-1, 1]^d$ and solve the following linear system:

$$\begin{bmatrix} \Phi_{00} & \Phi_{10} & \cdots & \Phi_{N_p 0} \\ \Phi_{01} & \Phi_{11} & \cdots & \Phi_{N_p 1} \\ \vdots & \vdots & \vdots & \vdots \\ \Phi_{0N_p} & \Phi_{1N_p} & \cdots & \Phi_{N_p N_p} \end{bmatrix} \begin{bmatrix} \tilde{u}_0 \\ \tilde{u}_1 \\ \vdots \\ \tilde{u}_p \end{bmatrix} = \begin{bmatrix} \sum_{i=0}^{N_p} \hat{u}_i \Phi_i\left(g^{-1}\left(\tilde{\xi}_0\right)\right) \\ \sum_{i=0}^{N_p} \hat{u}_i \Phi_i\left(g^{-1}\left(\tilde{\xi}_1\right)\right) \\ \vdots \\ \sum_{i=0}^{N_p} \hat{u}_i \Phi_i\left(g^{-1}\left(\tilde{\xi}_{N_p}\right)\right) \end{bmatrix}, \tag{29}$$

where $\Phi_{ij} = \Phi_i(\tilde{\xi}_j)$. We rewrite the above equation in matrix form as

$$\mathbf{A}\tilde{\mathbf{u}} = \hat{\mathbf{u}}. \tag{30}$$

Due to the hierarchical structure of the basis, $\mathbf{A}^{-1}$ exists for any $(N_p + 1)$ distinct points in $[-1, 1]^d$. When *h*-type refinement is implemented we divide the random space of a certain random dimension $\hat{\xi}_i$ into two equal parts. For example, if $\hat{\xi}_i$ corresponds to element $[\hat{a}, \hat{b}]$ in the original random space $[-1, 1]$, the elements $[\hat{a}, \frac{\hat{a}+\hat{b}}{2}]$ and $[\frac{\hat{a}+\hat{b}}{2}, \hat{b}]$ will be generated in the next level. However, due to the linearity of transformation, we do not have to perform such a map from the original random space, as we can just separate the random space of $\hat{\xi}_i$, which is $[-1, 1]$, to $[-1, 0]$ and $[0, 1]$. Therefore, the matrix $\mathbf{A}$ will be the same for every *h*-type refinement, and we only need to compute $\mathbf{A}^{-1}$ once and store it for future use. When refinement is needed, we can obtain $\tilde{\mathbf{u}}$ easily by a matrix–vector multiplication

$$\tilde{\mathbf{u}} = \mathbf{A}^{-1}\hat{\mathbf{u}}. \tag{31}$$

For a relatively small polynomial order ($p \leqslant 10$), the mapping cost is small.

Now we summarize the ME-gPC algorithm.

Algorithm 1

Step 1: construct a stochastic ODE/PDE system by gPC
Step 2: perform the decomposition of random space adaptively
  time step *i*: **from 1 to** N
    loop over all random elements
      if $\eta^\alpha J_k \geqslant \theta_1$, **then**

      if $r_n \geqslant \theta_2 \cdot \mathbf{max}_{j\,=\,\mathbf{1},\ldots,d} r_j,$ **then**
         split random dimension ξ_n **into two equal ones and generate**
         local random variables $\xi_{n,\mathbf{1}}$ **and** $\xi_{n,\mathbf{2}}$
      end if
    end if
    map information to the children random elements
    update the information of new elements by gPC
  end loop
 end time step
Step 3: postprocessing stage

3.5. Generalization

Let ζ be a general (i.e., non-uniform) random vector, whose components are IID random variables. Let ζ denote any component of ζ. We can approximate it by Legendre-chaos in the form

$$\zeta = \sum_{i=0}^{N_p} a_i \Phi_i(\xi), \tag{32}$$

where ξ is a *uniform* random variable. The procedure for such an approximation can be found in [4]. Note here that we need d IID uniform random variables to approximate all components of ζ. By expressing everything in terms of the Legendre-chaos, then we can employ ME-gPC in terms of ξ.

Another choice is to first decompose the random space of ζ. Assume that $u(\zeta)$ is a random field of ζ, then the mth moment of $u(\zeta)$ is

$$\mu_m(u) = \int_B u^m(\zeta) h(\zeta) \mathrm{d}\zeta, \tag{33}$$

where $h(\zeta)$ is the PDF. Suppose that we have decomposed the random space of ζ to elements B_i, $i = 1, 2, \ldots, N$. The above equation can be rewritten as

$$\mu_m(u) = \sum_{i=1}^{N} \int_{B_i} v_i u^m(\zeta) \frac{h(\zeta)}{v_i} \mathrm{d}\zeta, \tag{34}$$

where $v_i = \int_{B_i} h(\zeta) \mathrm{d}\zeta$. We can then express $h(\zeta)/v_i$ as a conditional PDF of ζ in B_i,

$$\bar{h}(\zeta \,|\, B_i) = \frac{h(\zeta)}{v_i}. \tag{35}$$

Then, the mth moment of $u(\zeta)$ can be expressed in the following form:

$$\mu_m(u) = \sum_{i=1}^{N} v_i \int_{B_i} u^m(\zeta) \bar{h}(\zeta \,|\, B_i) \mathrm{d}\zeta. \tag{36}$$

Now we can employ the first choice to approximate the conditional PDF $\bar{h}(\zeta \,|\, B_i)$ by uniform random variables ξ. Since we approximate $\bar{h}(\zeta \,|\, B_i)$ only in a subspace of ζ, we may use a smaller number of Legendre-chaos modes for a desired level of accuracy.

Finally, another choice is to construct orthogonal polynomials on-the-fly for arbitrary PDFs. This construction is under development (see [12]).

4. Numerical results

In this section, we first demonstrate the convergence of ME-gPC for an algebraic equation and a simple ODE. Next, we focus on issues related to discontinuities in random space and study the Kraichnan–Orszag problem. Subsequently, we present numerical results for the stochastic advection–diffusion equation. Finally, we demonstrate the *h*-type convergence of the decomposition of random space for the approximation of general random inputs.

4.1. A simple algebraic equation

We first revisit the following stochastic algebraic equation considered in [8]

$$cu = 1, \tag{37}$$

where c is a positive uniform random variable in $[a, b]$.

In Fig. 1, the *h*-type convergence is shown, with the mean on the left and variance on the right. Here we set $a = 2$ and $b = 3$. By a least-squares fit of the data, we obtain that the index of algebraic convergence is $2(p + 1)$ for both the mean and the variance, which is consistent with the theoretical estimates given in [8].

4.2. One-dimensional ODE

In this section we study the performance of ME-gPC for the following simple ODE equation studied with the original gPC in [4]

$$\frac{\mathrm{d}u}{\mathrm{d}t} = -\kappa(\omega)u, \quad u(0; \omega) = u_0, \tag{38}$$

where $\kappa(\omega) \sim U(-1, 1)$. The exact solution can be easily found as

$$u(t; \omega) = u_0 e^{-\kappa(\omega)t}. \tag{39}$$
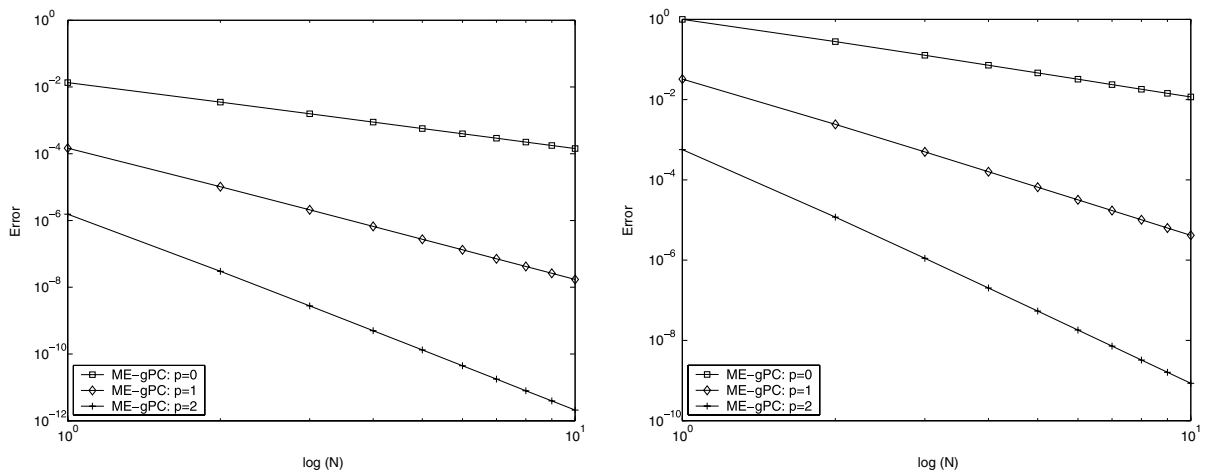
Fig. 1. *h*-type convergence for the algebraic equation. (left) Mean; (right) variance.
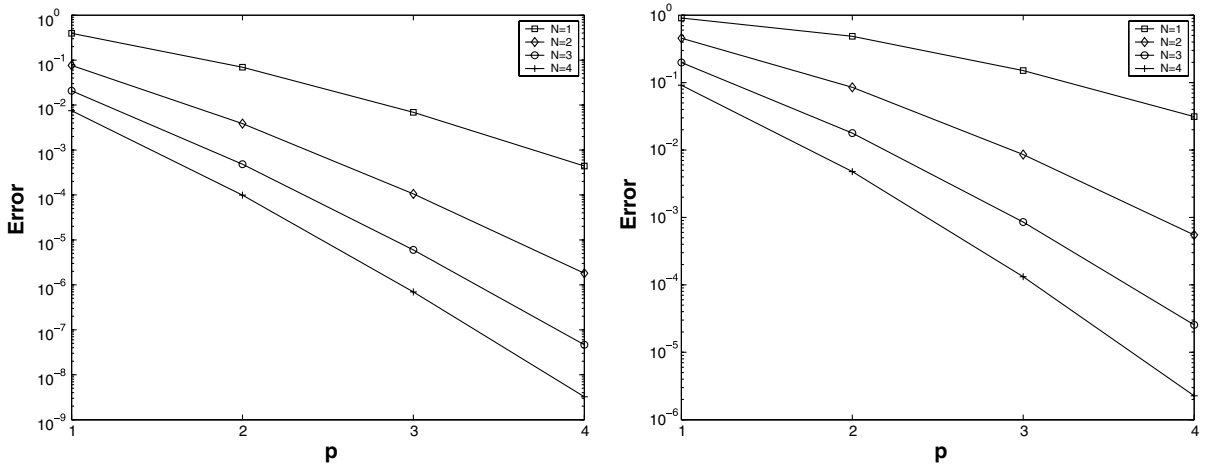
Fig. 2. Stochastic ODE: exponential convergence of ME-gPC with respect to polynomial order ($t = 5$). (left) Mean; (right) variance.

In Fig. 2, we show the exponential convergence of ME-gPC for different meshes. We can see that for greater number of equidistant random elements, not only is the error smaller, but the rate of convergence is much sharper. We show the algebraic convergence of ME-gPC in terms of element number N in Fig. 3. For this problem, the algebraic index of convergence is $2(p + 1)$ for both mean and variance, which means $\epsilon \sim O(N^{-2(p+1)})$. We have obtained a large algebraic index of convergence, which implies that random elements can influence the accuracy dramatically. In Fig. 4, the error evolution of gPC and ME-gPC is shown for two different levels of accuracy. Because the accuracy of exact solutions is set to be 10^{-10}, there is some oscillation at the beginning of the curves. It can be seen that when the error of gPC becomes big enough, θ_1 can trigger the decomposition of random space and the accuracy can then be improved significantly. In Fig. 5, we show how the number of random elements increases adaptively. Note here that the mesh can be non-uniform, because we only decompose the random elements in which the criterion is satisfied.
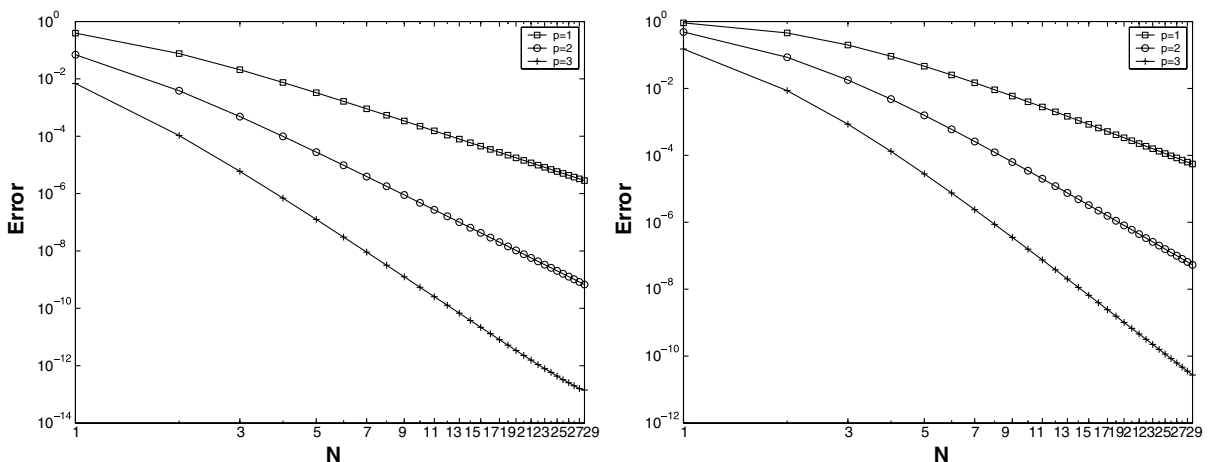
Fig. 3. Stochastic ODE: algebraic convergence of ME-gPC with respect to number of random elements ($t = 5$). (left) Mean; (right) variance.
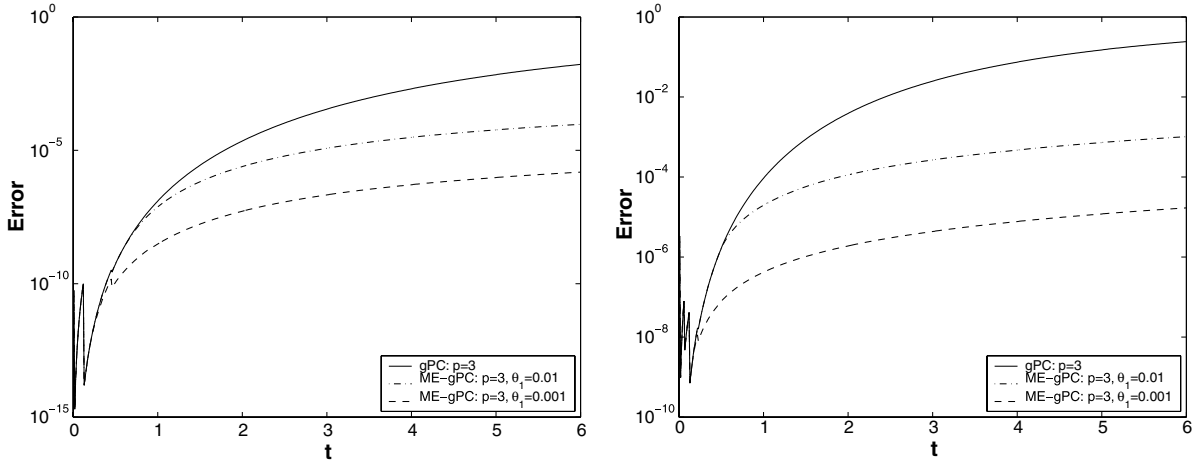
Fig. 4. Stochastic ODE: error evolution of gPC and ME-gPC with $\alpha = 1/2$. (left) Mean; (right) variance.

4.3. The Kraichnan–Orszag three-mode problem

It is well known that polynomial chaos fails in a short time for the so-called Kraichnan–Orszag three-mode problem [13]. In this section we first explain why this happens and subsequently we apply ME-gPC to effectively resolve this 40-year old open problem.

4.3.1. Why gPC fails

The Kraichnan–Orszag problem [13] is a nonlinear three-dimensional stochastic ODE system:
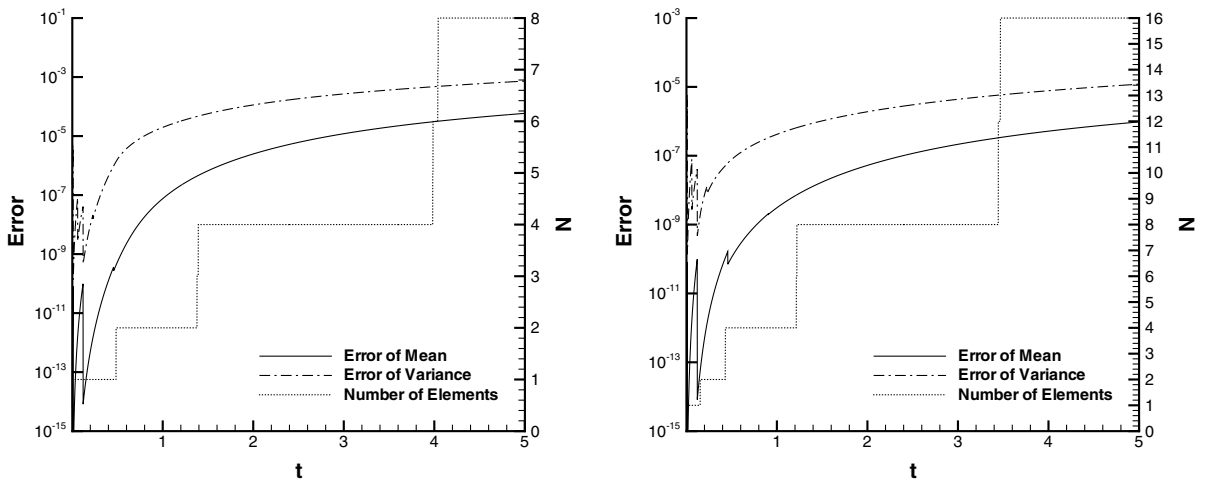
Fig. 5. Stochastic ODE: error (left axis) and number of random elements (right axis) with $\alpha = 1/2$. (left) $p = 3$, $\theta_1 = 0.01$; (right) $p = 3$, $\theta_1 = 0.001$.

$$\frac{dx_1}{dt} = x_2 x_3,$$
$$\frac{dx_2}{dt} = x_1 x_3,$$
$$\frac{dx_3}{dt} = -2x_1 x_2,$$

(40)

subject to stochastic initial conditions

$$x_1(0) = x_1(0;\omega), \quad x_2(0) = x_2(0;\omega), \quad x_3(0) = x_3(0;\omega).$$

(41)

We first check the deterministic solutions of Eq. (40). Given different initial conditions, deterministic solutions can be basically separated into four different groups g_i, $i = 1, 2, 3, 4$, which are shown in Fig. 6. All these four groups of solutions are periodic. If the initial conditions are located on the planes $x_1 = x_2$ and $x_1 = -x_2$, the corresponding solutions would stay on these two planes forever due to two fixed points $(0, 0, \sqrt{2x_1^2(0) + x_3^2(0)})$ and $(0, 0, -\sqrt{2x_1^2(0) + x_3^2(0)})$. By considering the properties of elliptic functions [14], we can obtain the analytic solutions of each group. Here we only give the analytic form of group g_1:

$$x_1 = P\,cn[q(t - t_0)], \quad x_2 = Q\,dn[q(t - t_0)], \quad x_3 = -R\,sn[q(t - t_0)],$$

(42)

where cn[·], sn[·] and dn[·] are Jacobi's elliptic functions and P, Q, R, q and t_0 are constants to be determined. We now substitute Eq. (42) into Eq. (40) to obtain

$$Pq = QR, \quad Qk^2 q = PR, \quad Rq = 2PQ,$$

(43)

where k is the modulus of elliptic functions. Since we have three initial conditions

$$P\,cn[q(t - t_0)] = x_1(0;\omega),$$
$$Q\,dn[q(t - t_0)] = x_2(0;\omega),$$
$$-R\,sn[q(t - t_0)] = x_3(0;\omega),$$

(44)

we have six equations with six unknowns P, Q, R, k, q and t_0. Thus, we have obtained the exact general solution of the Kraichnan–Orszag problem.
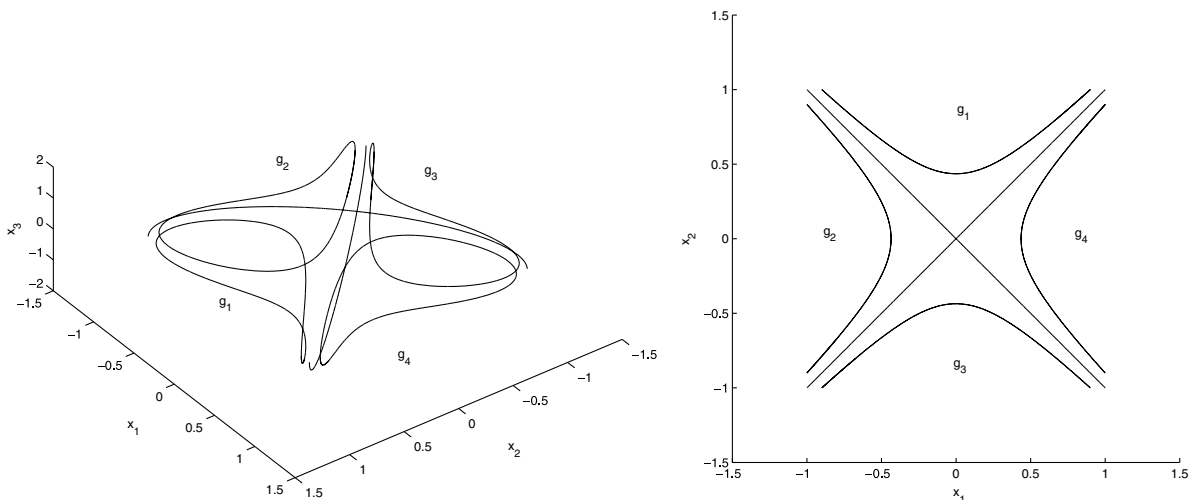
Fig. 6. Deterministic solutions of the Kraichnan–Orszag problem subject to different initial conditions. (left) 3D phase space; (right) 2D projection on x_1–x_2 plane.

We now consider the following initial conditions:

$$x_1(0) = \alpha + 0.01\xi, \quad x_2(0) = 1.0, \quad x_3(0) = 1.0, \tag{45}$$

where ξ is a uniform random variable and α is a constant. By solving Eqs. (43) and (44), we can determine the unknowns as

$$
\begin{aligned}
P^2 &= f^2(\xi) + \frac{1}{2}, \quad Q^2 = \frac{3}{2}, \quad R^2 = 2f^2(\xi) + 1, \\
p^2 &= 3, \quad k^2 = \frac{2}{3}f^2(\xi) + \frac{1}{3}, \quad t_0 = -\mathrm{dn}^{-1}\left[\frac{1}{Q}\right] \Big/ p,
\end{aligned}
\tag{46}
$$

where $f(\xi) = \alpha + 0.01\xi$.

Next we examine the Fourier expansions of Jacobi's functions:

$$
\begin{aligned}
\mathrm{sn}[u] &= \frac{2\pi}{kK}\left[\frac{q^{1/2}\sin z}{1-q} + \frac{q^{3/2}\sin 3z}{1-q^3} + \frac{q^{5/2}\sin 5z}{1-q^5} + \cdots\right], \\
\mathrm{cn}[u] &= \frac{2\pi}{kK}\left[\frac{q^{1/2}\cos z}{1+q} + \frac{q^{3/2}\cos 3z}{1+q^3} + \frac{q^{5/2}\cos 5z}{1+q^5} + \cdots\right], \\
\mathrm{dn}[u] &= \frac{\pi}{2K} + \frac{2\pi}{K}\left[\frac{q\cos 2z}{1+q^2} + \frac{q^2\cos 4z}{1+q^4} + \frac{q^3\cos 6z}{1+q^6} + \cdots\right],
\end{aligned}
\tag{47}
$$

where $q = q(\xi)$, $K = K(\xi)$ and $z = z(\xi, t)$. First, we can see that the frequency depends on the random variable ξ. It is well known that this will reduce the effectiveness of gPC as the initial phase difference will be amplified very fast as time increases. In Fig. 7, we show how the period of x_1 change as $x_1(0) \to 1$. We can see that the period of x_1 will increase to infinity as $x_1(0)$ goes to 1. Note here that if $x_1(0) = 1$, the initial point $(1,1,1)$ would be on the plane $x_1 = x_2$. Second, if q goes to 1, it is clear that we need more and more
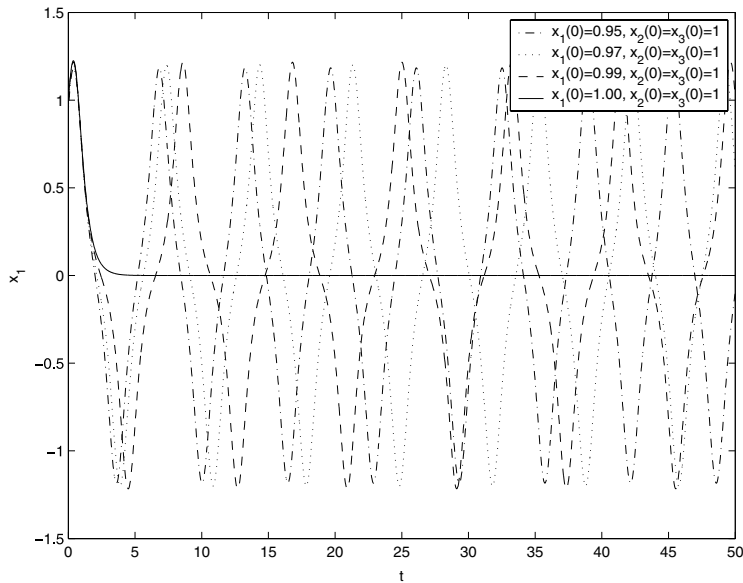
Fig. 7. Kraichnan–Orszag problem: several *deterministic* solutions of x_1 versus time corresponding to different initial conditions.

terms for the expansion of sn[u], which means that the order of polynomial chaos must increase correspondingly to resolve the solution.

From Eqs. (45) and (46) we can see that if ξ is uniform in $[-1, 1]$, x_1 is uniform in $[\alpha - 0.01, \alpha + 0.01]$ and the range (non-uniform) of $k(\xi)$ is $\left[\sqrt{\frac{2}{3}(\alpha - 0.01) + \frac{1}{3}}, \sqrt{\frac{2}{3}(\alpha + 0.01) + \frac{1}{3}}\right]$. Let k_r denote the upper bound of $k(\xi)$. It is clear that if $\alpha \to 0.99$, $k_r \to 1$. By the properties of elliptic functions, we know that $q \to 1$ when $k \to 1$. Thus, for the same degree of perturbation gPC should work less efficiently when $\alpha \to 0.99$, because $k(\xi)$ will be closer to 1. Now, we investigate four simple cases: $\alpha = 0.94$, 0.96, 0.98 and 0.99. For simplicity we only show the results for x_1, since the situation is similar for x_2 and x_3. In Fig. 8 we show how gPC fails when $\alpha \to 0.99$. It can be seen that in Fig. 8(a)–(d) the valid range of polynomial chaos with order $p = 6$ becomes shorter as α increases. If α is strictly less than 0.99 corresponding to $q < 1$, increasing the polynomial order can efficiently improve the results of polynomial chaos. For the cases (a)–(c), the results of polynomial chaos with order $p = 20$ agree very well with the results of Monte Carlo with 100,000 realizations. However, if $\alpha = 0.99$ is included, the periods of stochastic solutions will change from a finite value to infinity and increasing the polynomial order hardly improves the results for this case. It is shown in (d) that the
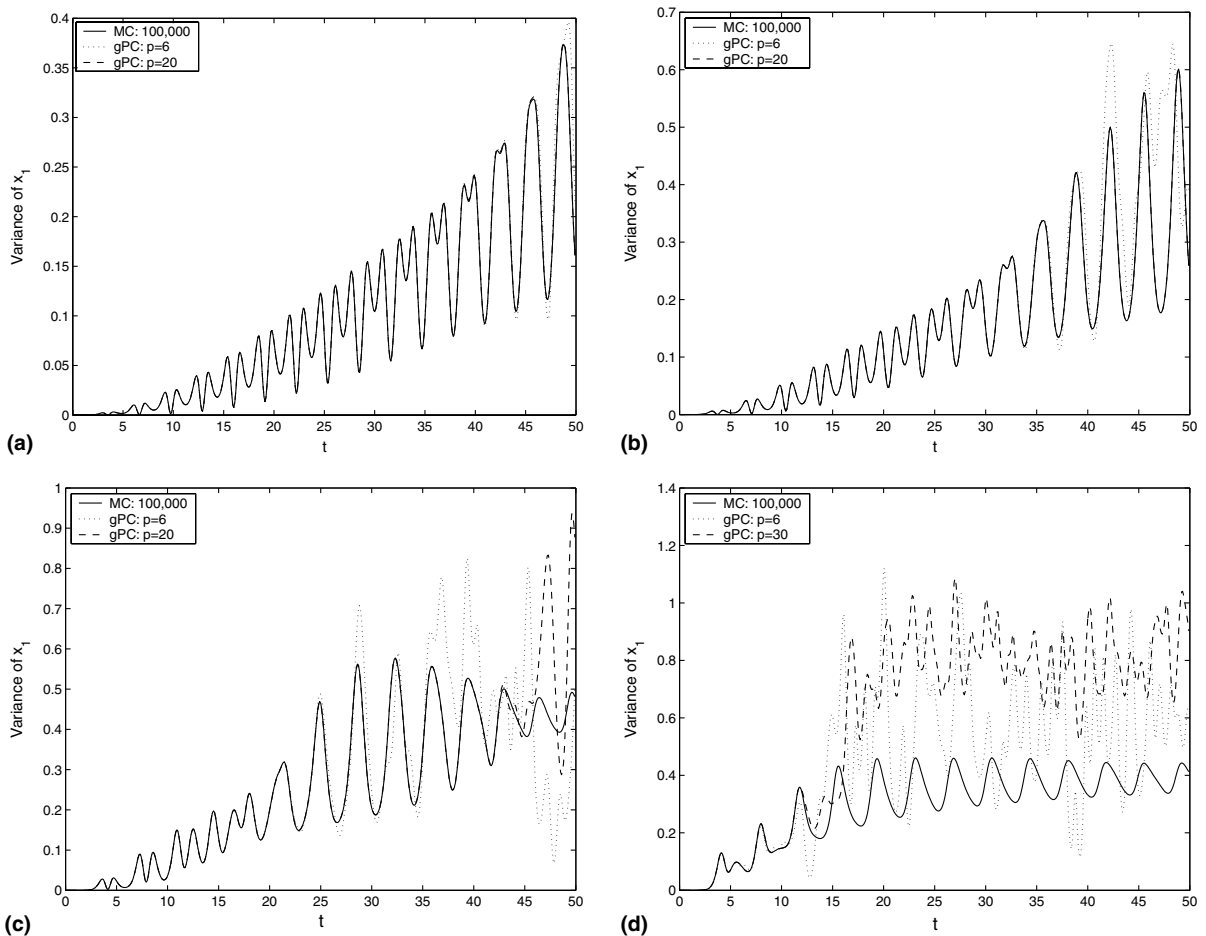
Fig. 8. Comparison of variance obtained from gPC and Monte Carlo simulations. (a) $\alpha = 0.94$; (b) $\alpha = 0.96$; (c) $\alpha = 0.98$; (d) $\alpha = 0.99$.

X. Wan, G.E. Karniadakis / Journal of Computational Physics 209 (2005) 617–642

correct part of the variance given by polynomial chaos with order $p = 30$ is almost the same with that given by polynomial chaos with order $p = 6$. Therefore, it is at the bifurcation point where gPC fails to converge.

In general, if the initial random data does not intersect with the planes $x_1 = x_2$ and $x_1 = -x_2$, we can improve the results of polynomial chaos by increasing the polynomial order, otherwise, polynomial chaos will diverge even after a short time of integration.

4.3.2. One-dimensional random input

Let us first study the random discontinuity of the Kraichnan–Orszag three-mode problem, which is introduced by one-dimensional random input. For computational convenience and clarity in the presentation we first perform the following transformation:

$$
\begin{bmatrix} y_1 \\ y_2 \\ y_3 \end{bmatrix} = \begin{bmatrix} \frac{\sqrt{2}}{2} & \frac{\sqrt{2}}{2} & 0 \\ -\frac{\sqrt{2}}{2} & \frac{\sqrt{2}}{2} & 0 \\ 0 & 0 & 1 \end{bmatrix} \begin{bmatrix} x_1 \\ x_2 \\ x_3 \end{bmatrix}. \tag{48}
$$

As a result, we will rotate the deterministic solutions by $\pi/4$ around to x_3 axis in the phase space. Now the new system is

$$
\begin{aligned}
\frac{\mathrm{d}y_1}{\mathrm{d}t} &= y_1 y_3, \\
\frac{\mathrm{d}y_2}{\mathrm{d}t} &= -y_2 y_3, \\
\frac{\mathrm{d}y_3}{\mathrm{d}t} &= -y_1^2 + y_2^2,
\end{aligned} \tag{49}
$$

subject to initial conditions

$$
y_1(0) = y_1(0;\omega), \quad y_2(0) = y_2(0;\omega), \quad y_3(0) = y_3(0;\omega). \tag{50}
$$

From now on, we will study this problem based on Eq. (49). Note that the discontinuity occurs at the planes $y_1 = 0$ and $y_2 = 0$ after the transformation. Gaussian random variables are used as random inputs in [13]. Here, we use *uniform* random variables since the discontinuity can be introduced similarly. Thus, we study the stochastic response subject to the following random input:

$$
y_1(0;\omega) = 1, \quad y_2(0;\omega) = 0.1\xi(\omega), \quad y_3(0;\omega) = 0, \tag{51}
$$

where $\xi \sim U(-1,1)$. Since the random initial data $y_2(0;\omega)$ can cross the plane $y_2 = 0$, we know from the aftermentioned discussion that gPC will fail for this case.

In Fig. 9, we show the evolution of the variance of y_1 within the time interval $[0, 30]$. For comparison we include the results given by gPC with polynomial order $p = 30$. It can be seen that comparing to the results given by Monte Carlo with 1,000,000 realizations, gPC with polynomial order $p = 30$ begins to lose accuracy at $t \approx 8$ and fails beyond this point while ME-gPC converges as θ_1 decreases. In Table 1, we show the maximum normalized error of the variance of y_1, y_2 and y_3 at $t = 30$ given by ME-gPC and the corresponding number of random elements. It is seen that when the threshold parameter θ_1 decreases, the accuracy becomes better and we can obtain almost $O(\theta_1)$ error. As we mentioned before, the reason that errors are usually bigger than θ_1 is due to the discontinuity which can reduce the convergence of gPC. It can be seen that for the same polynomial order we need more random elements to get a better accuracy; on the other hand, for the same θ_1 increasing the polynomial order can reduce the number of random elements.

In Fig. 10, we show four adaptive meshes. We can see that around the point $\xi = 0$ in random space of ξ, where the discontinuity occurs, the random elements are smallest, which means that the discontinuity can
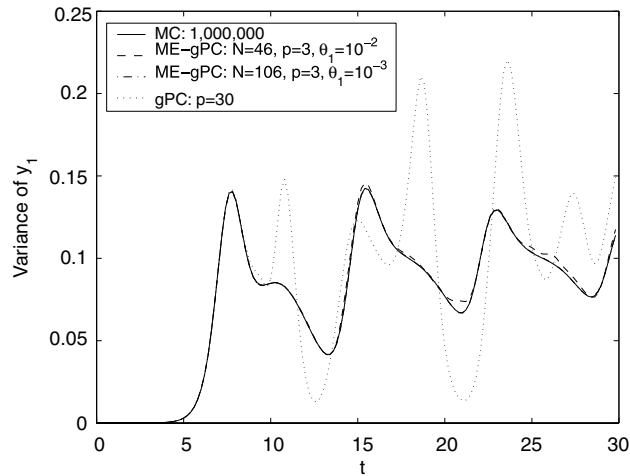
Fig. 9. Evolution of the variance of y_1 for one-dimensional random input.

Table 1
Maximum normalized errors of the variance of y_1, y_2 and y_3 at $t = 30$ with $\alpha = 1/2$

	$\theta_1 = 10^{-2}$		$\theta_1 = 10^{-3}$		$\theta_1 = 10^{-4}$		$\theta_1 = 10^{-5}$	
	N	Error	N	Error	N	Error	N	Error
$p = 3$	46	3.10e − 2	106	2.32e − 3	280	1.37e − 4	820	2.87e − 5
$p = 4$	36	9.90e − 2	74	3.24e − 3	138	3.45e − 4	286	2.31e − 5
$p = 5$	28	7.24e − 2	44	4.10e − 3	78	2.90e − 4	130	4.35e − 6

The results given by ME-gPC with $\theta_1 = 10^{-7}$ and polynomial order $p = 5$ are used as exact solutions.

be captured by small random elements. In Fig. 11, we show the errors of Monte Carlo and ME-gPC in terms of computational cost. The error is the L_∞ error of the variance of y_1 in the time interval $[8, 30]$, where gPC fails. To implement gPC, we need to apply Galerkin projection onto the chaos basis, resulting in the ensemble average $\langle \Phi_i \Phi_j \Phi_k \rangle$ of three basis modes. Here, we count the operations of $\langle \Phi_i \Phi_j \Phi_k \rangle$ for ME-gPC in order to estimate its cost. For Monte Carlo, the number of realizations is employed in the cost evaluation. Let n denote the number of operations. If the data in Fig. 11 are approximated by a first-order polynomial in a least-squares sense, we can obtain accuracy proportional to $n^{-0.49}$, $n^{-2.25}$, $n^{-2.99}$ and $n^{-4.24}$, respectively, for Monte Carlo and ME-gPC with polynomial order $p = 3$, $p = 4$ and $p = 5$, respectively. The decay rate for Monte Carlo is about $n^{-0.5}$ as expected. Comparing to Monte Carlo, the errors of ME-gPC show a much greater decay rate in terms of the cost. We can see that the speed-up increases for higher accuracy, which implies that ME-gPC is an efficient alternative to Monte Carlo for integration where high-order accuracy is required. In Fig. 12, we show the error contribution of each random element. Here we compare two criteria with $\alpha = 1/2$ and $\alpha = 1/4$. It is seen that the shape of error distribution is like an isosceles triangle, i.e., a "Gibbs-like" behavior. On the apex of the triangle is the largest error contribution, where discontinuity occurs. The error contribution decreases quickly away from the discontinuity, since $\eta_k J_k \sim \eta_k^{1-\alpha} \theta_1$ and η_k is much smaller on the smooth part. Because gPC loses accuracy as time increases, the error contribution of each element will become larger with time and more random elements with relative errors of O(1) would appear around the discontinuity point. For a smaller α, the error contribution near the discontinuity decreases much faster.
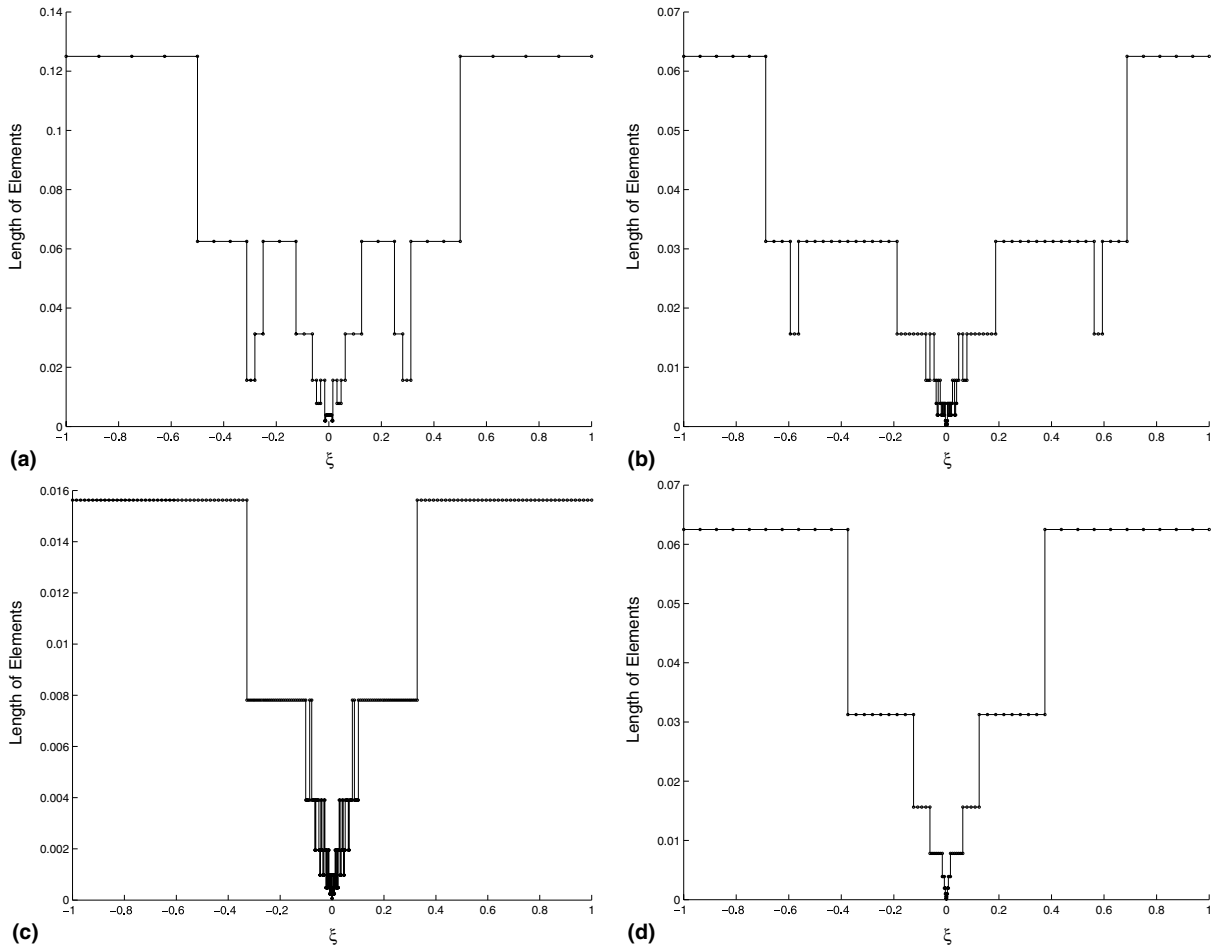
Fig. 10. Adaptive meshes for the 1D random input with $\alpha = 1/2$. (a) $\theta_1 = 0.01$, $p = 3$; (b) $\theta_1 = 0.001$, $p = 3$; (c) $\theta_1 = 0.0001$, $p = 3$; (d) $\theta_1 = 0.0001$, $p = 5$.

4.3.3. Two-dimensional random input

In this section we use ME-gPC to study the Kraichnan–Orszag problem with two-dimensional random input

$$y_1(0;\omega) = 1, \quad y_2(0;\omega) = 0.1\xi_1(\omega), \quad y_3(0;\omega) = \xi_2(\omega), \tag{52}$$

where ξ_1 and ξ_2 are uniform random variables in $[-1, 1]$.

In Fig. 13, we show the evolution of the variance of y_1, y_2 and y_3 and an adaptive two-dimensional mesh. For comparison we include the result given by gPC with polynomial order $p = 10$. It can be seen that gPC with polynomial order $p = 10$ begins to diverge around $t \approx 4$ while ME-gPC with $p = 5$ Legendre-chaos shows good convergence to the results given by Monte Carlo with 1,000,000 realizations. From the final refined mesh, we can see that the results are more sensitive to ξ_1, because ξ_1 can cross the plane $y_2 = 0$ where the discontinuity occurs. Note here that the discontinuity domain is a line. In Fig. 14, we show the error of Monte Carlo and ME-gPC in terms of computational cost. Here we regard the results given by ME-gPC with $\theta_1 = 10^{-6}$ and $p = 5$ as exact solutions. From the empirical fit we obtain an accuracy proportional to $n^{-0.50}$, $n^{-1.72}$ and $n^{-2.56}$, respectively, for Monte Carlo and ME-gPC with $p = 3$ and $p = 5$. It is seen that
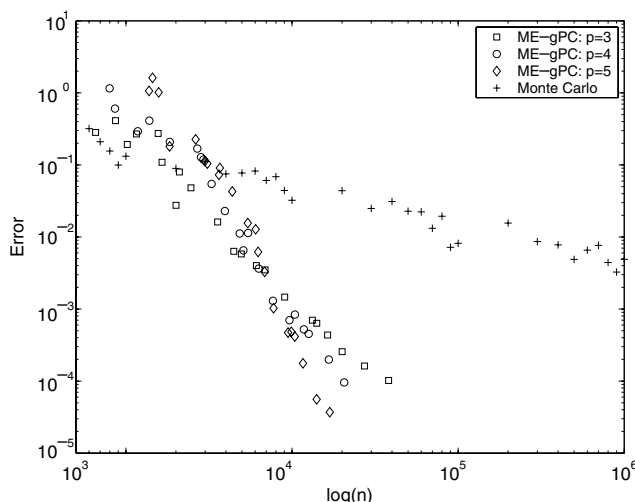
Fig. 11. Error versus cost of Monte Carlo simulations and ME-gPC with different polynomial orders (based on the L_∞ error of the variance of y_1 in the time interval $[8, 30]$). Here we only count the average number of operations in one time step.

ME-gPC is much faster than Monte Carlo for higher accuracy. Comparing to the 1D case, however, the decay rate of relative error becomes smaller because both the random dimension and the discontinuity domain become larger.

4.3.4. Three-dimensional random input

In this section we use ME-gPC to study the Kraichnan–Orszag problem with three-dimensional random input

$$y_1(0) = \xi_1(\omega), \quad y_2(0) = \xi_2(\omega), \quad y_3(0) = \xi_3(\omega), \tag{53}$$

where ξ_1, ξ_2 and ξ_3 are uniform random variables in $[-1, 1]$.

In Fig. 15, we show the evolution of variance. Due to the symmetry of y_1 and y_2 in Eq. (49) and the symmetry of $y_1(0)$ and $y_2(0)$ in the random inputs, the variances of y_1 and y_2 are the same. Here we only show the results for y_1 and y_3. It can be seen that gPC diverges around $t \approx 1$ and fails subsequently while ME-gPC shows good convergence as before. For this case, the random space $[-1, 1]^3$ of random inputs contains both $y_1 = 0$ and $y_2 = 0$ where discontinuities occur. Comparing to the case with 2D random inputs, the discontinuity domain is much larger. Thus, it is more difficult to resolve the 3D case. Based on the results given by ME-gPC with polynomial order 3 and $\theta_1 = 10^{-5}$, the L_∞ errors of the variance of y_1 in the time interval $[1.5, 6]$ are 0.16% and 0.21%, respectively, for Monte Carlo with 1,000,000 realizations and ME-gPC with polynomial order $p = 3$ and $\theta_1 = 10^{-3}$. Thus, these two errors are comparable. For this case, the speed-up of ME-gPC is much lower compared to the 2D problem. From the previous results, we know that this speed-up would increase for higher accuracy, but the increasing speed would be lower comparing to the 1D and 2D cases. In Fig. 16, we show the evolution of the random elements generated. It can be seen that to maintain the accuracy, the element number has to increase at a speed about 100 elements per time unit.

In summary, ME-gPC shows good convergence when solving the Kraichnan–Orszag problem and it can achieve a desired accuracy at a cost much lower than Monte Carlo. However, ME-gPC loses efficiency for problems with strong discontinuity and high-dimensional random inputs, because the number of random elements has to increase fast to maintain a desired accuracy.
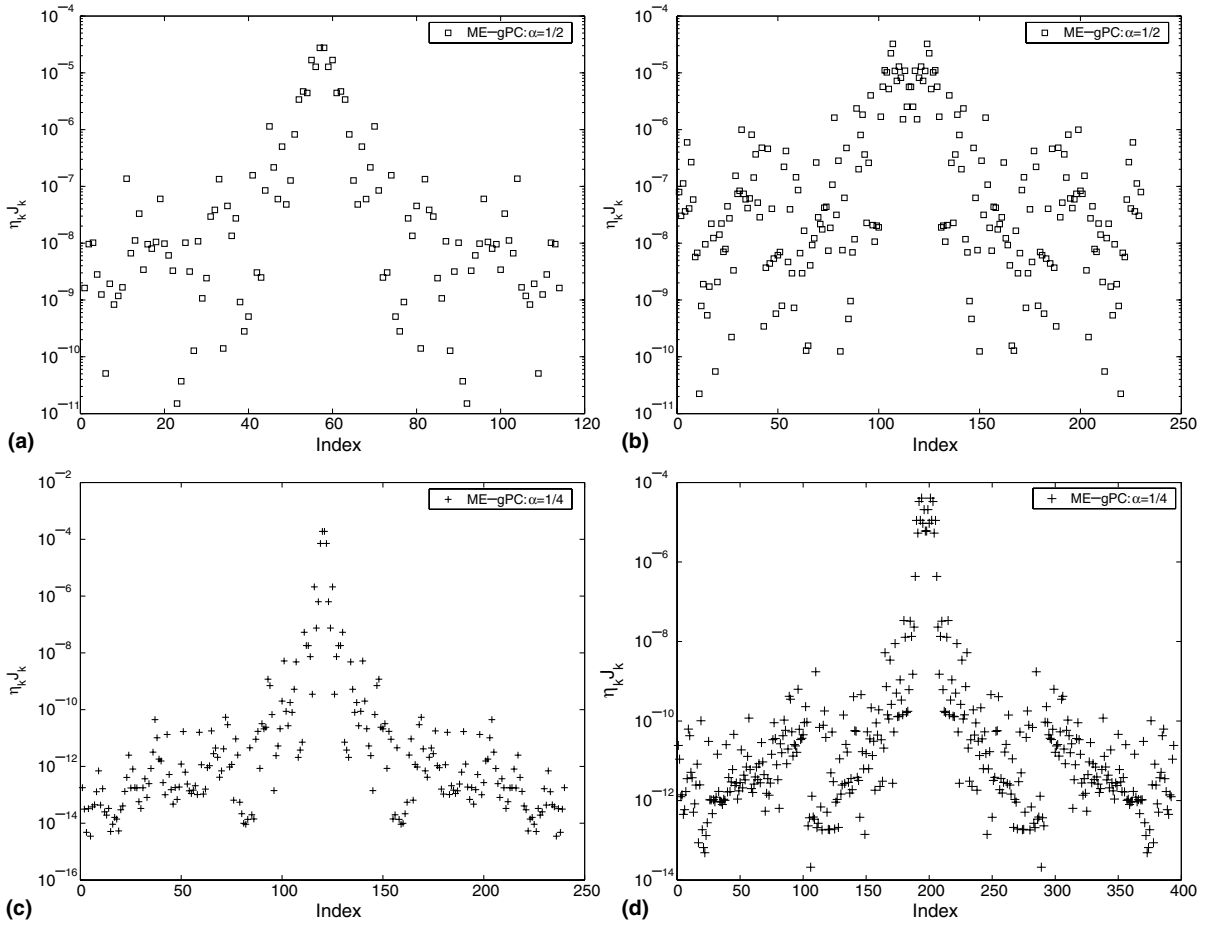
Fig. 12. Error contribution of each random element given by two criteria with different α. $\theta_1 = 10^{-4}$ and $p = 5$. (a) $\alpha = 1/2$, $t = 50$; (b) $\alpha = 1/2$, $t = 100$; (c) $\alpha = 1/4$, $t = 50$; (d) $\alpha = 1/4$, $t = 100$.

4.4. Stochastic advection–diffusion equation

In this section we consider the 2D stochastic advection–diffusion equation first studied in [15] using gPC

$$\frac{\partial \phi}{\partial t}(\mathbf{x}, t; \omega) + \mathbf{u}(\mathbf{x}; \omega) \cdot \nabla \phi = v \nabla^2 \phi, \tag{54}$$

where $\mathbf{u}(\mathbf{x}; \omega) = (y + a(\omega), -x - b(\omega))$. For the initial condition

$$\phi(\mathbf{x}, 0; \omega) = e^{-[(x-x_0)^2 + (y-y_0)^2]/2\lambda^2}, \tag{55}$$

the corresponding exact solution can be found as

$$\phi_e(\mathbf{x}, t; \omega) = \frac{\lambda^2}{\lambda^2 + 2vt} e^{-(\hat{x}^2 + \hat{y}^2)/2(\lambda^2 + 2vt)}, \tag{56}$$
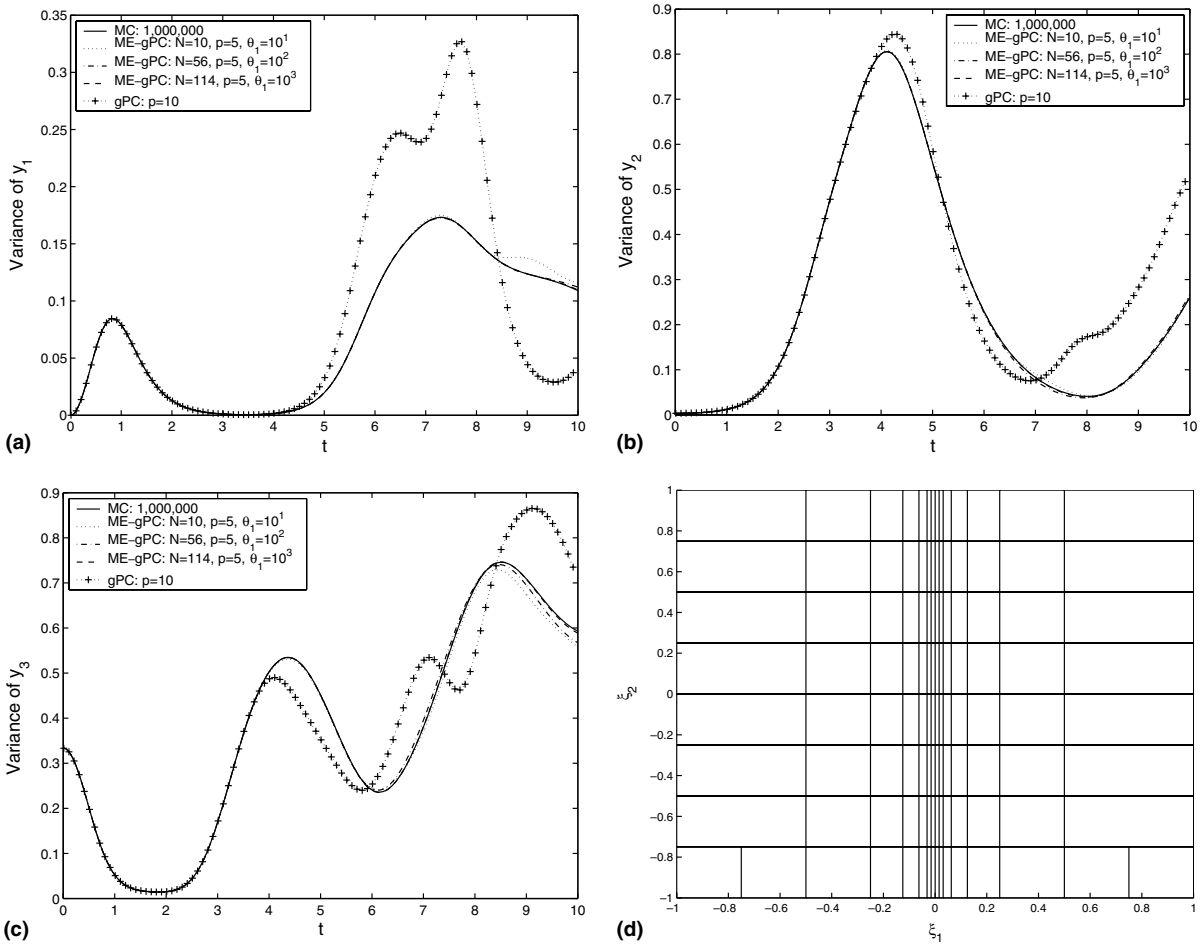
Fig. 13. The Kraichnan–Orszag problem with 2D random inputs. $\alpha = 1/2$, $\theta_1 = 0.1, 0.01, 0.001$ and $\theta_2 = 0.1$. (a) $\sigma_{y_1}^2$; (b) $\sigma_{y_2}^2$; (c) $\sigma_{y_3}^2$; (d) adaptive mesh for $\theta_1 = 0.001$ and $p = 5$.

where λ is a constant and

$$\begin{cases} \hat{x} = x + b(\omega) - (x_0 + b(\omega)) \cos t - (y_0 + a(\omega)) \sin t, \\ \hat{y} = y + a(\omega) + (x_0 + b(\omega)) \sin t - (y_0 + a(\omega)) \cos t. \end{cases}$$

Here we let $a(\omega) = b(\omega) = 0.1\xi$, where $\xi \sim U(-1, 1)$. In Fig. 17, we show the convergence of ME-gPC with equidistant elements, p-type convergence on the left and h-type convergence on the right. We can see that ME-gPC not only exhibits exponential converge but shows an increasing convergence rate as the number of elements increases. For h-type convergence, we only show the results of up to four random elements, since the error decreases quickly. It is seen that the index of algebraic convergence is related to the polynomial order, where the decay rate corresponding to higher polynomial order is very large. More experiments are required to estimate the exact convergence rate numerically.
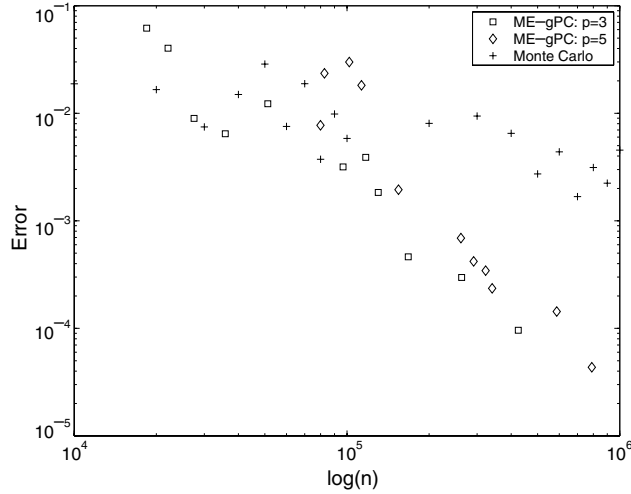
Fig. 14. Error versus cost of Monte Carlo simulations and ME-gPC with 2D Legendre-chaos (based on the L_∞ error of the variance of y_1 in the time interval $[4, 10]$). Here we only count the average number of operations in one time step.
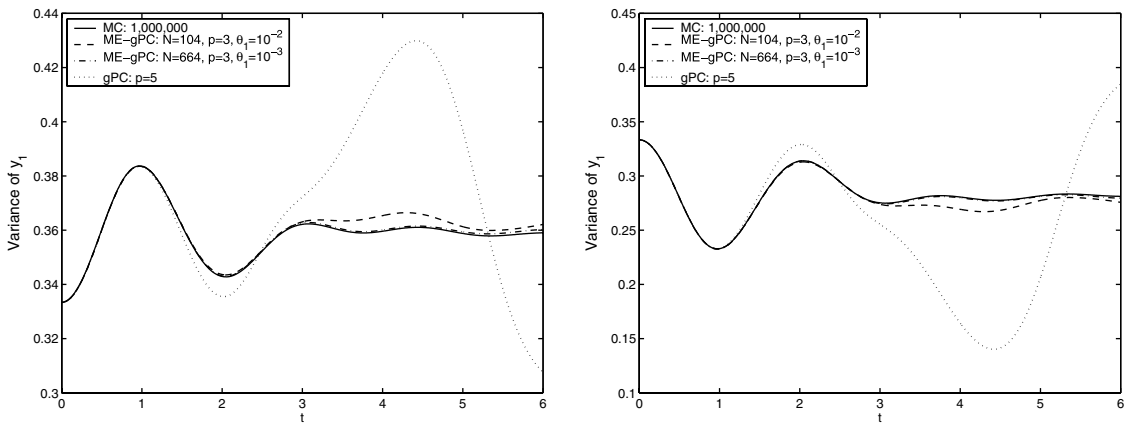
Fig. 15. Evolution of variance for the 3D Kraichnan–Orszag problem. $\theta_2 = 10^{-1}$. (left) $\sigma_{y_1}^2 = \sigma_{y_2}^2$; (right) $\sigma_{y_3}^2$.

4.5. Approximation of a Beta-type random variable by Legendre-chaos

Finally, we demonstrate how to generalize ME-gPC to other random variables. We consider a Beta-type random variable Y of distribution $\mathscr{B}e(\alpha, \beta)$, where $\mathscr{B}e(\alpha, \beta)$ is the conventional definition of Beta distribution in the domain $[0, 1]$

$$f(y) = \frac{1}{B(\alpha + 1, \beta + 1)} y^\alpha (1 - y)^\beta, \quad \alpha, \beta > -1, \ 0 \leqslant y \leqslant 1. \tag{57}$$

Here $B(\cdot, \cdot)$ denotes the Beta function. Let $\alpha = 1$ and $\beta = 0$, then the PDF of Y is

$$f(y) = 2y. \tag{58}$$
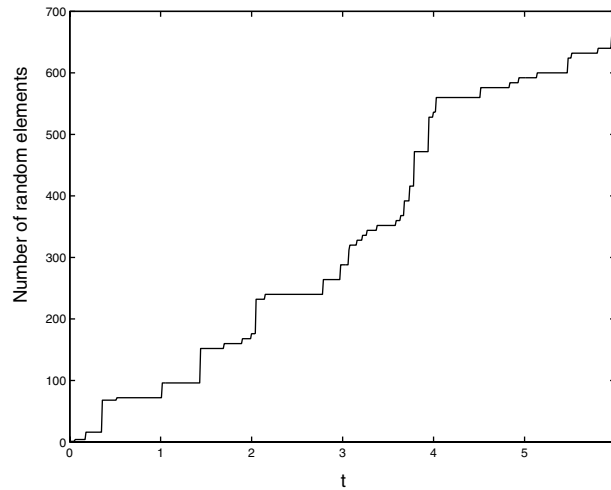
Fig. 16. Evolution of the element number for the 3D Kraichnan–Orszag problem. $\theta_1 = 10^{-3}$.
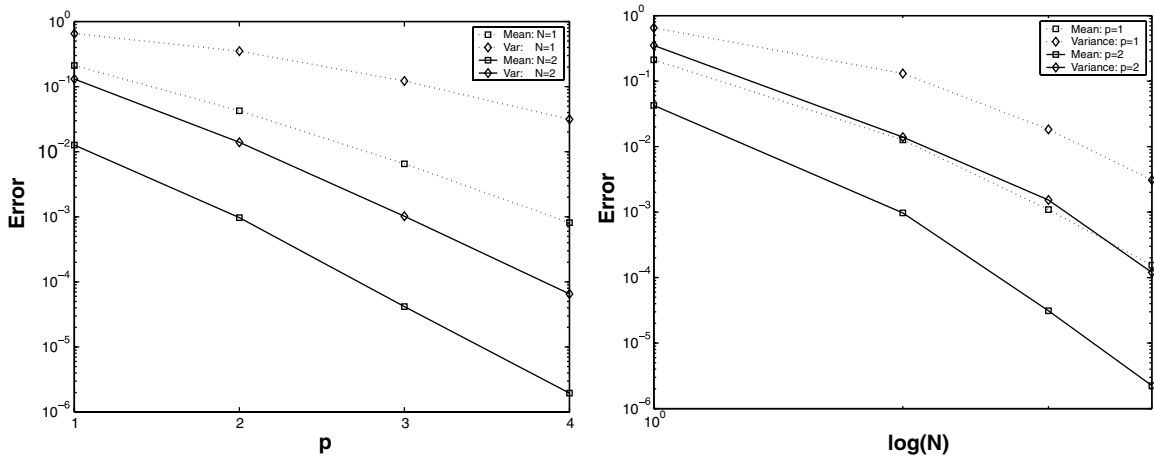
Fig. 17. Convergence of gPC and ME-gPC for 2D advection–diffusion equation with $a(\omega) = b(\omega) = 0.1\xi$ at $t = 3.14$. (left) p-type convergence; (right) h-type convergence.

Since the uniform random variable used in Legendre-chaos is defined in the domain $[-1,1]$, we introduce a new random variable X defined in $[-1,1]$ with the transformation $Y = \frac{1}{2}X + \frac{1}{2}$. Thus, the PDF of X is

$$f(x) = \frac{1+x}{2}. \tag{59}$$

Let us assume that the random space $[-1,1]$ of X is separated into N equal elements $[a,b]$. In each element we define a new random variable X_i, $i = 1,2,\ldots,N$ with a corresponding PDF

$$f_i(x_i) = \frac{1}{\int_{[a,b]} f(t)\mathrm{d}t} \frac{1+x_i}{2} = \frac{1+x_i}{(1+a/2+b/2)(b-a)}. \tag{60}$$

Subsequently, we use a uniform random variable τ to express X_i. A transformation of variables in probability space shows that

$$\frac{1}{2}d\tau = f_i(x_i)dx_i = dF(x_i), \tag{61}$$

where F is the distribution function of X_i. Thus, we can obtain

$$\frac{1+\tau}{2} = F(x_i). \tag{62}$$

After inverting the above equation, we obtain

$$x_i = F^{-1}\left(\frac{1+\tau}{2}\right) = \sqrt{(1+a/2+b/2)(b-a)(1+\tau)+(1+a)^2} - 1. \tag{63}$$

Then X_i can be expressed by Legendre-chaos as

$$X_i = \sum_{j=0}^{p} x_{i,j}\Phi_j(\tau) \tag{64}$$

with

$$x_{i,j} = \frac{1}{\langle \Phi_j^2 \rangle} \int_{[-1,1]} F^{-1}\left(\frac{1+\tau}{2}\right)\Phi_j(\tau)\frac{1}{2}d\tau. \tag{65}$$

Now each X_i has been approximated by a uniform random variable τ; thus, we can implement ME-gPC in each element when solving a stochastic differential equation with random inputs related to X. Here, we only check the accuracy of $\mu_2(X) = \mathbb{E}[X^2]$. We compute $\mu_2(X)$ using Eq. (36). In Fig. 18, we show the error of $\mu_2(X)$ in terms of the element number N. It is seen that an algebraic convergence with index -4 is obtained, which means that the error is proportional to N^{-4}. This specific value is dictated by the accuracy of the mapping that we performed and can be improved if higher accuracy is desired. Therefore, the decomposition of random space can also be used to approximate a general random variable in order to improve
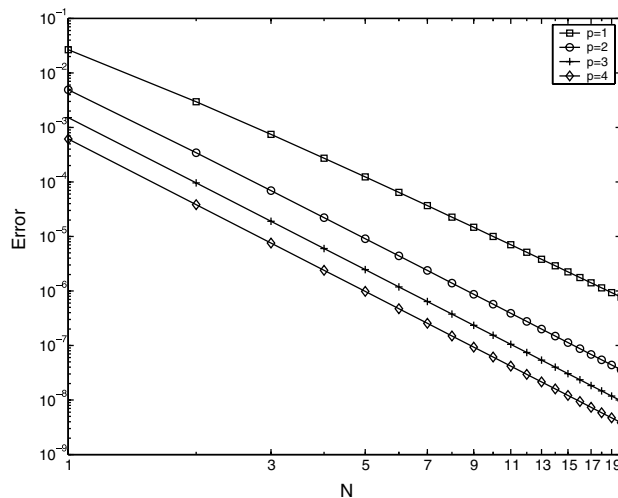
Fig. 18. Error of $\mu_2(X)$ for a Beta distribution.

accuracy. Furthermore, we can use a low-order Legendre-chaos when implementing ME-gPC in each random element.

5. Summary

We have extended the gPC framework, first presented in [4,5], to a multi-element formulation (ME-gPC). The new approach can maintain a desired accuracy by adaptively decomposing the random space of random inputs when a simple criterion is satisfied. Correspondingly, the efficiency and especially the effectiveness of gPC is significantly improved.

To investigate the performance of ME-gPC we present several examples including stochastic algebraic, ordinary and partial differential equations. In particular, we address errors in *long-time integration* and in *discontinuities* in random space. An example with one-dimensional ODE shows that ME-gPC can achieve *h-p* type of convergence. The error of long-term integration is efficiently controlled by the criterion we developed for the adaptive decomposition of random space. Subsequently, we explain why gPC fails for the classical Kraichnan–Orszag three-mode problem, and study it with ME-gPC for different random inputs. The results indicate that ME-gPC can capture accurately the discontinuity by the decomposition of random space. In particular, the adaptive criterion can be used to select the most sensitive random dimension, and thus make the decomposition of random space more efficient. A two-dimensional advection–diffusion equation is also simulated by ME-gPC. The results suggest that ME-gPC could also improve the efficiency of gPC for stochastic PDEs. More results for stochastic problems of incompressible flow using the ME-gPC method presented here are included in [12]. Finally, we approximate a random variable of Beta distribution by Legendre-chaos, thus demonstrating how to deal with general *non-uniform* random inputs.

ME-gPC is efficient for stochastic systems, which contain no or small subdomains of discontinuities, such as the 1D ODE model and the Kraichnan–Orszag problem with 1D or 2D random inputs. However, its efficiency is reduced significantly by the rapidly increasing number of random elements for problems with high-dimensional random inputs and large discontinuities, as in the Kraichnan–Orszag problem with 3D random inputs. Such problems require new approaches in constructing appropriate low-dimensional approximations, as in the work of [16,17].

Acknowledgment

References

[1] N. Wiener, The homogeneous chaos, Am. J. Math. 60 (1938) 897–936.
[2] R.G. Ghanem, P. Spanos, Stochastic Finite Elements: a Spectral Approach, Springer, New York, 1991.
[3] R.G. Ghanem, J. Red-Horse, Propagation of uncertainty in complex physical systems using a stochastic finite elements approach, Physica D 133 (1999) 137–144.
[4] D. Xiu, G.E. Karniadakis, The Wiener–Askey polynomial chaos for stochastic differential equations, SIAM J. Sci. Comput. 24 (2) (2002) 619–644.
[5] D. Xiu, G.E. Karniadakis, Modeling uncertainty in flow simulations via generalized polynomial chaos, J. Comput. Phys. 187 (2003) 137–167.
[6] O.P.L. Maitre, H.N. Njam, R.G. Ghanem, O.M. Knio, Uncertainty propagation using Wiener–Haar expansions, J. Comput. Phys. 197 (2004) 28–57.

 [7] O.P.L. Maitre, H.N. Njam, R.G. Ghanem, O.M. Knio, Multi-resolution analysis of Wiener-type uncertainty propagation schemes, J. Comput. Phys. 197 (2004) 502–531.
 [8] M.K. Deb, I. Babuška, J.T. Oden, Solution of stochastic partial differential equations using Galerkin finite element techniques, Comput. Methods Appl. Mech. Eng. 190 (2001) 6359–6372.
 [9] R.H. Cameron, W.T. Martin, The orthogonal development of nonlinear functionals in series of Fourier–Hermite functionals, Ann. Math. 48 (1947) 385.
[10] M. Loeve, Probability Theory, fourth ed., Springer, New York, 1977.
[11] G.E. Karniadakis, S.J. Sherwin, Spectral/*hp* Element Methods for CFD, Oxford University Press, Oxford, 1999.
[12] X. Wan, Multi-element generalized polynomial chaos for differential equations with random imputs: algorithms and applications, Ph.D. Thesis, Brown University (in preparation).
[13] S.A. Orszag, L.R. Bissonnette, Dynamical properties of truncated Wiener–Hermite expansions, Phys. Fluids 10 (12) (1967) 2603–2613.
[14] D.F. Lawden, Elliptic Functions and Applications, Springer, New York, 1989.
[15] X. Wan, D. Xiu, G.E. Karniadakis, Stochastic solutions for the two-dimensional advection–diffusion equation, SIAM J. Sci. Comput. 26 (2) (2004) 578–590.
[16] C. Schwab, R.A. Todor, Sparse finite elements for elliptic problems with stochastic data, Numer. Math. 95 (2003) 707–734.
[17] R.A. Todor, Numerical analysis of Galerkin FEM for stochastic elliptic PDEs, Ph.D. Thesis, ETHZ (in preparation).